Sonochemical Deposition of Silver Nanoparticles on Silica Spheres

V. G. Pol,[†] D. N. Srivastava,[†] O. Palchik,[†] V. Palchik,[‡] M. A. Slifkin,[‡] A. M. Weiss,[‡] and A. Gedanken*[,†]

Department of Chemistry, Bar-Ilan University, Ramat-Gan, 52900, Israel, and Department of Electronics, Jerusalem College of Technology, Jerusalem, 91160, Israel

Received August 29, 2001. In Final Form: January 24, 2002

Silver nanoparticles with an average size of ∼5 nm were deposited on the surface of preformed silica submicrospheres with the aid of power ultrasound. Ultrasound irradiation of a slurry of silica submicrospheres, silver nitrate, and ammonia in an aqueous medium for 90 min under an atmosphere of argon to hydrogen (95:5) yielded a silver−silica nanocomposite. By controlling the atmospheric and reaction conditions, we could achieve the deposition of metallic silver on the surface of the silica spheres. The resulting silver-deposited silica submicrosphere samples were characterized with X-ray diffraction, transmission electron microscopy, differential scanning calorimetry, energy-dispersive X-ray analysis, high-resolution transmission electron microscopy, high-resolution scanning electron microscopy, photoacoustic spectroscopy, and Fourier transform infrared, UV−visible, and X-ray photoelectron spectroscopy.

Introduction

The preparation and characterization of nanosized metal clusters have been active areas of investigation.[1] Aside from their very high surface area, these particles possess chemical and physical properties that are distinct from those of both the bulk phase and individual molecules and have potential for applications in optics, optoelectronics, catalysis, and so forth. In view of the importance of the surface structure of nanoparticles on their properties, much effort has been invested in order to create new classes of materials through the modification of surface structure. Recent achievements include the development of methods for the preparation of coated nanoparticles, including metal/semiconductor (metal on semiconductor),[2] semiconductor/semiconductor,[3] and semiconductor/metal composite nanoparticles.[4] Several investigators have reported on the deposition of silver nanoparticles on silica spheres. They used a variety of techniques including the inverse micelle method,[5] nonionic reverse micelles,[6] pretreatment steps in electroless plating,[7] and the sol−gel method.[8] In the present work, we describe an additional method, that is, an ultrasound-driven synthesis. This method has previously been used to disperse gold nanoparticles within the pores of mesoporous silica.[9] Power ultrasound effects chemical changes due to cavitation phenomena involving the formation, growth, and collapse of bubbles.[10] The silica spheres used in our experiment as the substrate for the silver deposition were made by the Stöber method. Stöber's silica submicrospheres[11] are obtained by the base-catalyzed hydrolysis of tetraethyl orthosilicate (TEOS). The silica spheres qualify as hard spherical substrates for the following reasons: (a) narrow size distribution can be achieved over a wider range; (b) their surface silanol composition and the extent of hydrogen bonding can be modified by thermal treatment to change their reactivity; (c) silanol groups can form covalent links; and (d) the isotropic interactions in an aqueous or organic suspension, which help to form ordered arrays on substrates. With the continuing interest in the controlled synthesis and characterization of ceramic and metal−ceramic nanoparticles, we have explored the effect of power ultrasound on ceramic materials such as silica microbeads and alumina gel,[12] as well as on the deposition of various nanoparticles, such as CdS,[13] iron/iron oxides,[14] and Eu_2O_3.[15] In this report, we present results related to the deposition of silver nanoparticles on submicrospherical silica. We also demonstrate our ability to determine whether the deposited material will be silver oxide or silver. When argon gas was bubbled through the slurry for 4 h prior to sonication to expel any dissolved oxygen/air, formation of Ag_2O was suppressed. All reactions were carried out in a reducing atmosphere of an Ar/H_2 mixture.

Experimental Section

1. Preparation of Substrate. Amorphous submicrospheres of silica in the size range of 325−350 nm were synthesized by base-catalyzed hydrolysis of TEOS, as described by Stöber et al.[11] Silica submicrospheres thus obtained were washed extensively with ethanol in a centrifuge and dried under vacuum at room temperature. The silica submicrospheres were heated at 600 °C for 3 h prior to use in the sonochemical reaction, to remove surface OH groups, thus preventing coagulation of the spheres with each other.[8,13]

* To whom correspondence should be addressed. E-mail: gedanken@mail.biu.ac.il.

[†] Department of Chemistry, Bar-Ilan University.

[‡] Department of Electronics, Jerusalem College of Technology.

(1) Lewis, L. N. *Chem. Rev.* **1993**, *93*, 2693−2730.

(2) Honma, I.; Sano, T.; Komiyama, H. *J. Phys. Chem.* **1993**, *97* (25), 6692−6695.

(3) Kortan, A. R.; Hull, R.; Opila, R. L. *J. Am. Chem. Soc.* **1990**, *112*, 1327−1332.

(4) Neuendort, R.; Quentin, M.; Keiling, U. *J. Chem. Phys.* **1996**, *104*, 6348.

(5) Lianos, P.; Thomas, J. K. *J. Colloid Interface Sci.* **1987**, *117*, 505−510.

(6) Zhang, Z. B.; Cheng, H. M.; Ma, J. M. *J. Mater. Sci. Lett.* **2001**, *20*, 439−440.

(7) Kobayashi, Y.; Salgueirino-Maceiraa, V.; Liz-Marzan, L. M. *Chem. Mater.* **2001**, *13*, 1630−1633.

(8) Shibata, S.; Aoki, K.; Yano, T.; Yamane, M. *J. Sol.-Gel Sci. Technol.* **1998**, *11*, 279−287.

(9) Chen, W.; Cai, W. P.; Liang, C. H.; Zhang, L. D. *Mater. Res. Bull.* **2001**, *136*, 335−342.

(10) *Ultrasound*: *Its Chemical, Physical and Biological Effects*; Suslick, K. S., Ed.; VCH: Germany, 1988.

(11) Stöber, W.; Fink, A.; Bohn, E. *J. Colloid Interface Sci.* **1968**, *26*, 62−69.

(12) Ramesh, S.; Koltypin, Y.; Gedanken, A. *J. Mater. Res.* **1997**, *12*, 3271−3277.

(13) Dhas, N. A.; Gedanken, A. *Appl. Phys. Lett.* **1998**, *72* (20), 2514−2516.

(14) Ramesh, S.; Prozorov, R.; Gedanken, A. *Chem. Mater.* **1997**, *9*, 2996−3004.

(15) Ramesh, S.; Minti, H.; Reisfeld, R.; Gedanken, A. *Opt. Mater.* **1999**, *13*, 67−70.

10.1021/la0155552 CCC: $22.00
Published on Web 03/03/2002

Table 1. Experimental Conditions for the Preparation of the Samples[a]

sample	bubbling duration	annealing	form	XRD composite
1			A	
2	4 h, Ar		A	
1h		100 °C, 3 h	C	Ag/Ag_2O
2h	4 h, Ar	100 °C, 3 h	C	Ag

[a] A = amorphous; C = crystalline. All the reactions were carried out under a reduced atmosphere of an Ar/H_2 mixture.

2. Sonochemical Deposition of Silver Nanoparticles. The annealed silica submicrospheres (225 mg) and 212 mg of silver nitrate were added to 100 mL of distilled water in a sonication cell, and the cell was attached to the sonicator horn under flowing argon. Argon gas was bubbled through the slurry for 4 h prior to sonication to expel dissolved oxygen/air. The sonication of the slurry with the high-intensity ultrasound radiation was carried out for 90 min by direct immersion of the titanium horn (Sonics and Materials VCX 600 sonifier, 20 kHz, 40 W/cm^2) in a sonication cell, under a flow of an argon/hydrogen mixture (95:5). A 7−10 mL portion of 24% (wt) aqueous ammonia was added in drops during the sonication. A sonication cell was placed in an acetone cooling bath, with a temperature of 15−20 °C maintained during the sonication. The product was washed thoroughly (twice) with doubly distilled deoxygenated water and then with ethanol in an inert glovebox. The product was then dried in a vacuum and stored under argon. The same reaction was also conducted without removing the oxygen/air from the sonication cell. We also carried out a reaction without addition of ammonia while maintaining all other conditions as before. Crystallization of the as-prepared product was carried out by heating a small amount of the sample in a boat crucible at a temperature of 100 °C under a flow of argon gas, for 3 h. All of the manipulations of the silver-coated silica submicrospheres were performed inside the glovebox, to prevent the formation of any traces of silver oxide. The reaction conditions and X-ray diffraction characterization data are summarized in Table 1.

3. Characterization. The X-ray diffraction patterns of the product were measured with a Bruker AXS D* Advance Powder X-ray diffractometer (using Cu Kα = 1.5418 Å radiation). The particle morphology and the nature of its adherence to silica were studied with transmission electron microscopy, which was done on a JEOL-JEM 100 SX microscope, working at a 100 kV accelerating voltage. High-resolution scanning electron microscope (HR-SEM) images were obtained using an LEO Gemini 982 field emission gun SEM (FEG-SEM) operating at a 4 kV accelerating voltage. High-resolution transmission electron microscope (HR-TEM) images were obtained using a JEOL-3010 set to a 300 kV accelerating voltage. A conventional CCD video camera, with a spatial resolution of 768 × 512 pixels, was used to digitize the micrographs, which were then processed using Digital Micrograph software. The elemental composition of the material was analyzed by energy-dispersive X-ray analysis (JEOL-JSM 840 scanning electron microscope). Differential scanning calorimetric analysis of the sample in a crimped aluminum crucible was carried out up to a temperature of 500 °C, using a Mettler (DSC-301) instrument under a flowing stream of nitrogen, at a heating rate of 10 °C/min. Absorption spectroscopy was carried out in the wavelength region of 300−800 nm, on a LKB Biochem (Ultraspec II 4050 UV−visible spectrophotometer).

Photoacoustic spectroscopy measurements were conducted employing a homemade instrument which is based on one which was described elsewhere,[16] but with completely updated software. The photoacoustic method consists of illuminating the sample by chopped monochromatic light in an airtight cell connected to a microphone. The light is absorbed and converted to heat. The chopped heat then flows to the surface of the sample whence it produces an acoustic wave. The wave is detected with a lock-in voltmeter. The signal thus acquired as a function of wavelength is normalized against the absorption of carbon black powder, the 100% absorber. The instrument operates over the wavelength region 300−800 nm. The spectrum is independent of the nature of the sample, unlike reflectance and absorption spectroscopy where the nature of the surface and sample morphology can have a marked effect on the spectrum. It is particularly useful for particulate matter, which causes turbidity and scattering so that conventional absorption spectroscopy is not very useful. This method is completely nondestructive. The photoacoustic spectra show much better resolved features than the absorption spectra. Due to the saturation phenomenon of the photoacoustic signal observed in very black samples, current samples were diluted with MgO powder. The ratio of the Ag/SiO_2 powder to MgO was 9:1. Fourier transform infrared spectroscopy was carried out on a Nicolet Impact 410 FTIR spectrometer. X-ray photoelectron spectra were measured with an AXIS, HIS 165, ULTRA (Kratos Analytical).

(16) Slifkin, M. A.; Luria, L.; Weiss, A. M. *Proc. SPIE-Int. Soc. Opt. Eng.* **1998**, *3110*, 481−487.

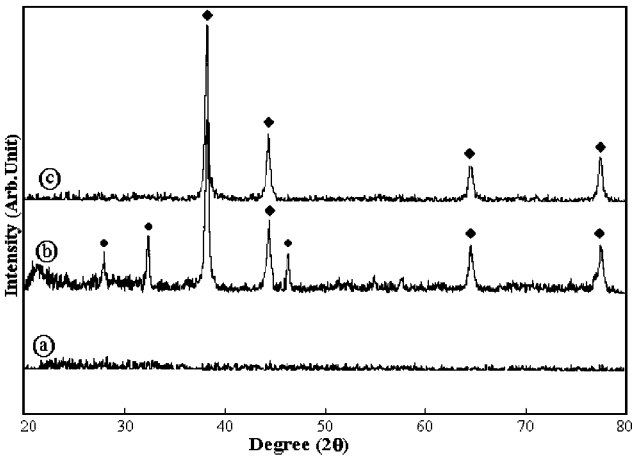

Figure 1. X-ray diffraction patterns of (a) samples 1 and 2; (b) sample 1h (◆ indicates the peaks of metallic Ag, and ● indicates the peaks of Ag_2O); (c) sample 2h (◆ indicates the peaks of metallic Ag).

Results and Discussion

1. X-ray Diffraction (XRD). In Figure 1a, the X-ray diffraction patterns of samples 1 and 2 are shown. The amorphous nature of the products is demonstrated by the absence of any diffraction peaks. The XRD diffraction patterns of both materials are the same. The XRD results for the heated samples are shown in Figure 1b,c for the 1h and 2h samples, respectively. When argon gas was not bubbled before the sonication of the sample (for sample 1h), two phases are observed in the XRD measurements (see Figure 1b). These are the cubic Ag (PDF: 4-783) and hexagonal Ag_2O (PDF: 42-0874) phases. For the compound (sample 2h), only the metallic silver phase is observed (see Figure 1c). On the basis of this observation, we presume that the bubbling of the solution prior to the sonication is required in order to obtain a pure silver phase.

2. Electron Microscopy Studies (TEM). Figure 2a shows the transmission electron micrographs of pre-prepared submicrospherical silica particle substrates, which were used in this study. The silica submicrospheres have a narrow size distribution, with their diameter in the 325−350 nm range. The TEM micrographs of the silica spheres deposited with amorphous nanoparticles (sample 1) are shown in Figure 2b. The TEM micrographs for the unheated samples (samples 1 and 2) are identical. In this case, the silica spheres were coated with a uniform amorphous layer. Except for a few amorphous 10−12 nm agglomerates, small crystalline particles were not seen, even at the highest resolution. These measurements lead us to conclude that the absence of peaks in the XRD data of samples 1 and 2 is due to the amorphous nature of the layer, and these particles are not X-ray amorphous. In the case of the heated samples (samples 1h and 2h), all

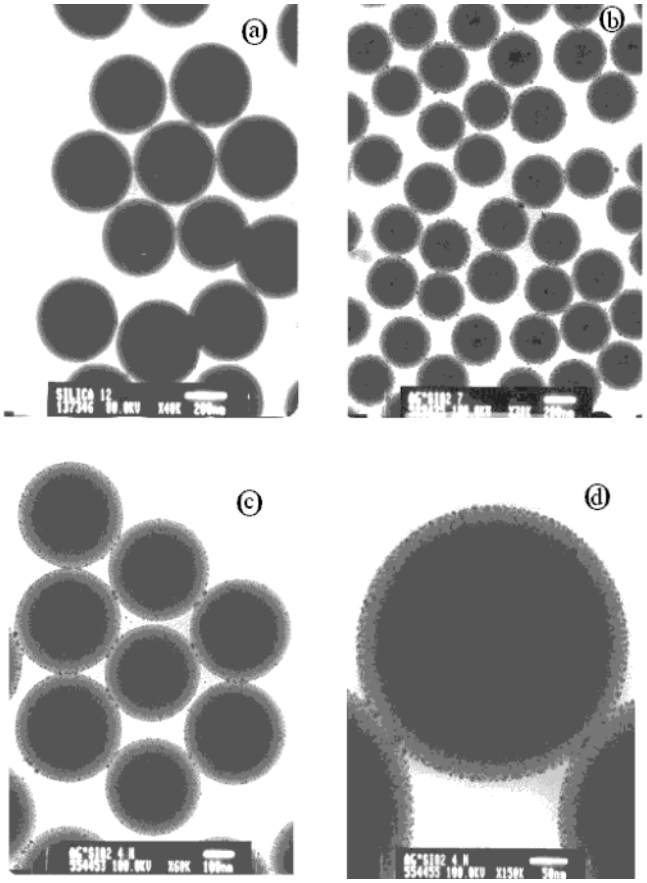

Figure 2. Transmission electron micrographs of (a) the bare substrate silica submicrospheres, (b) sample 1, (c) crystalline silver nanoparticles deposited on silica submicrospheres, sample 2h, and (d) a single submicrosphere shown at a high resolution, sample 2h.

of the silica submicrosphere surfaces are uniformly covered with silver nanosized particles. The TEM micrograph of the one of the crystallized samples is shown in Figure 2c.

Here, we could not identify whether the silver nanoparticles, which are deposited on silica submicrospheres, are oxidized or not. More than 90% of the particles have a diameter of approximately 4−5 nm. Sometimes, a few of the silver nanoparticles were trapped between two silica spheres having a larger particle size of approximately 8−10 nm. The amount of silver used for deposition was reduced in an attempt to avoid agglomeration of silver nanoparticles. When that was done, nonuniform deposition of silver nanoparticles was observed.

In Figure 2d, a single submicrosphere of silica deposited with silver nanoparticles is shown at a higher resolution (sample 2h). The higher resolution TEM micrographs show that silver nanoparticles in the 4−5 nm size range uniformly covered the surface of the silica submicrospheres.

The HR-SEM micrograph of sample 2h is shown in Figure 3 (in the inset a low-resolution image is shown). Due to the limit of the resolution, only large silver nanoparticles can be seen on the silica surface (approximate diameter of 10 nm). Therefore, HR-TEM was used to study individual small nanoparticles on the silica surface. In the HR-TEM micrograph of sample 2h, shown in Figure 4, the image was recorded along the [200] zone (the image was acquired at Scherezer defocus). We can clearly observe that the nanoparticle has perfect cubic arrangements of the atoms, which is in agreement with a cubic lattice of the metallic silver (PDF: 4-783). The

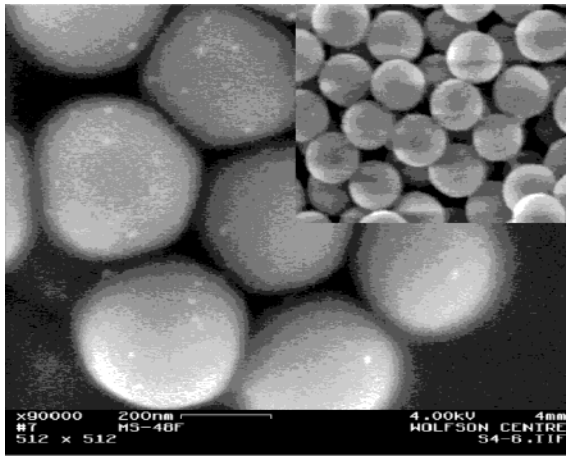

Figure 3. Scanning electron micrograph of sample 2h; white dots on the silica surface are big (∼10 nm) silver nanoparticles (inset: low-resolution image; horizontal lines on the inset image are due to the sample's charging).

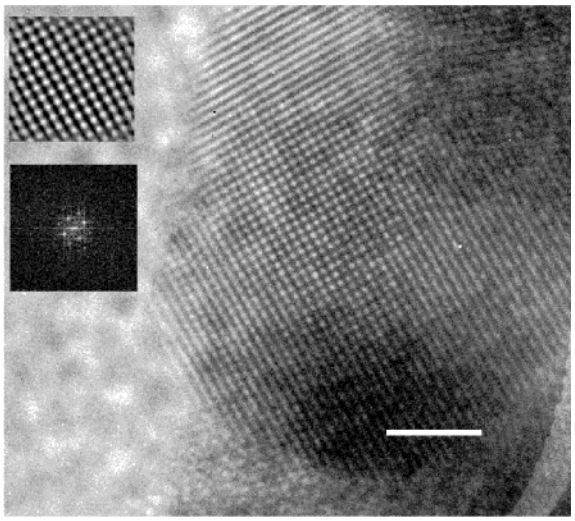

Figure 4. High-resolution TEM of sample 2h (the bar is equal to 2.1 nm). Insets: in the left upper corner, the fast Fourier transform filtered image of the lattice, and below that, the computer-generated diffraction pattern of the same lattice image.

distance between lattice planes is equal to 0.207 nm, which is very close to the distance of the (200) planes obtained from the XRD (0.2044 nm). No oxide layer was observed on the surface of these nanoparticles (more than 50 particles were examined).

3. Differential Scanning Calorimetry (DSC). Figure 5 shows the DSC curve (sample 2) for silver nanoparticles deposited on silica submicrospheres. The curves for both samples (samples 1 and 2) were very similar. The sample shows a broad endothermic peak in the region of 70−130 °C, which indicates the loss of adsorbed species and water molecules from the surface of the particles. The amorphous-to-crystalline transition of the silver nanoparticles coated on submicrospherical silica occurred at ∼312 °C, as indicated by the exotherm in the DSC spectrum (the onset of this peak at 270 °C and the end point at 370 °C). This peak was assigned to the crystallization of large silver particles (approximately 10 nm). Salkar and et al.[17] reported that the amorphous-to-crystalline transition of the silver nanoparticles occurs at 340 °C. On the other

(17) Salkar, R. A.; Jeevanandam, P.; Aruna, T.; Koltypin, Y.; Gedanken, A. *J. Mater. Chem.* **1999**, *9*, 1333−1335.

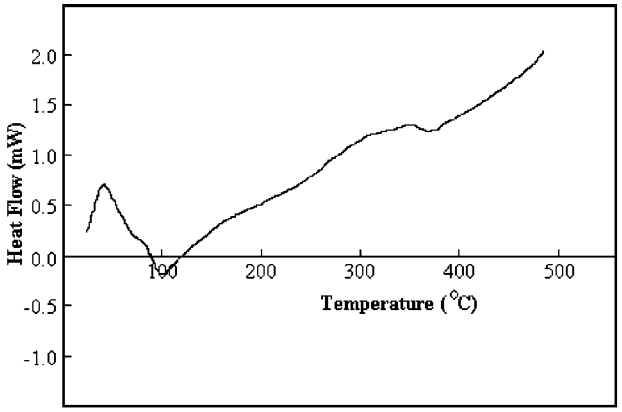

Figure 5. DSC spectrum of the as-prepared silver nanoparticles coated on submicrospherical silica (sample 2).

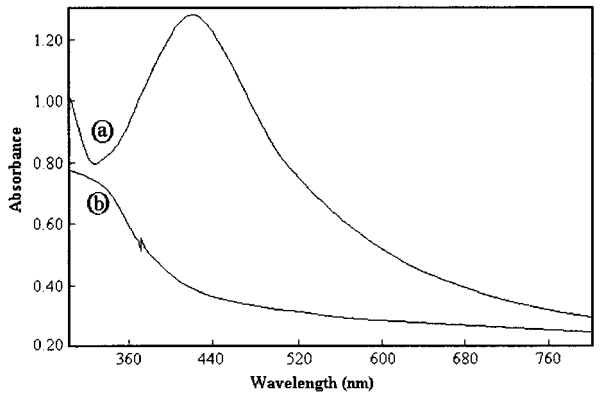

Figure 6. Absorption spectrum of an aqueous solution containing (a) crystalline silver nanoparticles deposited on silica submicrospheres (sample 2h) and (b) sample 1h.

hand, the crystallization of the amorphous small particles (1−4 nm) anchored on the silica surface occurs at a much lower temperature, at about 100 °C, and a weak exothermic shoulder is observed at 110 °C. The onset of this peak begins at temperatures lower than 100 °C, but this region of the exothermic peak is invisible due to its overlap with a broad endothermic peak due to water adsorption. This conclusion is supported by the XRD measurements, which show that annealing the as-prepared samples at 100 °C suffices for their crystallization. We propose that the drastic lowering of the crystallization temperature (312 to ∼100 °C) is due not to the size effect but rather to the anchoring of the silver atoms and the formation of a chemical bond with the silica. The cooling cycle and second heating cycle were featureless (data not shown).

4. Energy-Dispersive X-ray Analysis (EDAX). The presence of silver, silicon, and oxygen in the coated materials was examined with EDAX measurements. The EDAX spectrum was also used to obtain a quantitative estimate of the Ag and Ag/Si ratio. For the light elements such as oxygen, only a rough estimate could be done because EDAX is a bulk analysis, and oxygen from the silica spheres also contributes to the oxygen signal. Therefore, the Ag/O ratio could not be estimated from EDAX spectra. The silver, silicon, and Ag/Si ratio in all samples were identical (not heated and heated as well). The silver content in all the samples was about 8.5%. This value is close to the molar ratio of $AgNO_3/SiO_2$ in the starting solution.

5. UV−Visible Absorption Spectra. The UV−visible absorption spectrum of sample 2h, shown in Figure 6a, demonstrates the formation of silver nanoparticles, in agreement with the XRD measurements. These nanoparticles exhibit an intense, broad absorption peak around 415 nm, due to surface plasmon excitation. Surface plasmon excitation is a phenomenon that exists most commonly at the interface between a metal and a dielectric material, such as air and water.[18] The resonance is characteristic of colloidal metal particles, which are large enough (R > 1 nm) to exhibit bulk metallic properties.[19] The full width at half-maximum of this peak is approximately equal to 100 nm, which corresponds to the 5 nm average diameter of the silver nanoparticles.[19] Again, this is in agreement with our TEM measurements.

For sample 1h, no peaks were observed, even though some silver is present in this sample (see Figure 6b). This may be due to the relatively low sensitivity of the UV−vis absorption method.[20]

6. Photoacoustic Spectroscopy (PAS) Studies. In our previous work, the PAS method was used to study semiconductor nanoparticles, in order to measure their electronic properties (e.g., band gap).[21−23] As far as we know, there are only a few published studies where PAS was used to measure surface plasmon resonance (SPR),[24−26] and none of these papers described SPR measurements of small nanoparticles of the size described in this report. PAS may be very useful for the study of such particles, because in the case of analogous semiconductors, nanoparticle PAS was a superior technique, relative to other optical methods such as diffuse reflectance and absorption spectroscopy.[27,28]

The electronic properties of the products were studied by measurement of the optical absorption spectra (interband transitions) using photoacoustic spectroscopy (see Figure 7a,b). From previous studies using UV−vis absorption, it is known that the height and position of the peaks depend on various parameters: (1) the amount of Ag (affects the height of the peak);[8] (2) particle size (increased diameter causes a red shift);[29] (3) packing density of the particles (increased packing density causes a red shift);[24] and (4) oxidation level of the particles (increased oxidation level causes a blue shift).[30] The PAS spectrum of sample 2h shows two peaks (see Figure 7a), at 429 and 460 nm. This result indicates that two kinds of nanoparticles were present in the sample: very small ones, probably with a diameter of 2−4 nm (corresponding to the peak at 429 nm); and larger particles, with a diameter approximately equal to 10 nm. This result is consistent with TEM, DSC, and other measurements, as well as with the HR-SEM images, where only a few large (∼10 nm) dispersed particles are visible (see Figure 3). The PAS spectrum of sample 1h is shown in Figure 7b.

(18) *Optical effects associated with small particles*; Barber, P. W., Chang, R. K., Eds.; World Scientific: Singapore, 1988.
(19) Arnold, G. W.; Borders, J. A. *J. Appl. Phys.* **1997**, *48*, 1488−1496.
(20) Palchik, O.; Kerner, R.; Gedanken, A.; Weiss, A. M.; Slifkin, M. A.; Palchik, V. *J. Mater. Chem.* **2001**, *11*, 874−878.
(21) Rosencwaig, A. *Photoacoustics and photoacoustic spectroscopy*; Academic Press: New York, 1980.
(22) Grisaru, H.; Palchik, O.; Gedanken, A.; Palchik, V.; Slifkin, M. A.; Weiss, A. N.; Hacohen, Y. R. *Inorg. Chem.* **2001**, *40*, 4814−4815.
(23) Avivi, S.; Palchik, O.; Palchik, V.; Slifkin, M. A.; Weiss, A. M.; Gedanken, A. *Chem. Mater.* **2001**, *13*, 2195−2200.
(24) Seiler, H.; Haas, H.; Ocker, B.; Kortje, K. H. *Faraday Discuss.* **1991**, *92*, 121−128.
(25) Harata, A.; Shen, Q.; Sawada, T. *Annu. Rev. Phys. Chem.* **1999**, *50*, 193−219.
(26) Negm, S.; Talaat, H. *Solid State Commun.* **1992**, *84*, 133−137.
(27) Reich, I.; Diaz, P.; Marin, E. *Phys. Status Solidi B* **2000**, *220*, 305−308.
(28) Mandelis, A. *J. Therm. Anal.* **1991**, *37*, 1065−1101.
(29) Zhengxin, L.; Honghong, W.; Hao, L. *Appl. Phys. Lett.* **1998**, *72*, 1823−1825.
(30) Weiping, C.; Huicai, Z.; Zhang, L. *J. Appl. Phys.* **1998**, *83* (3), 1705−1710.

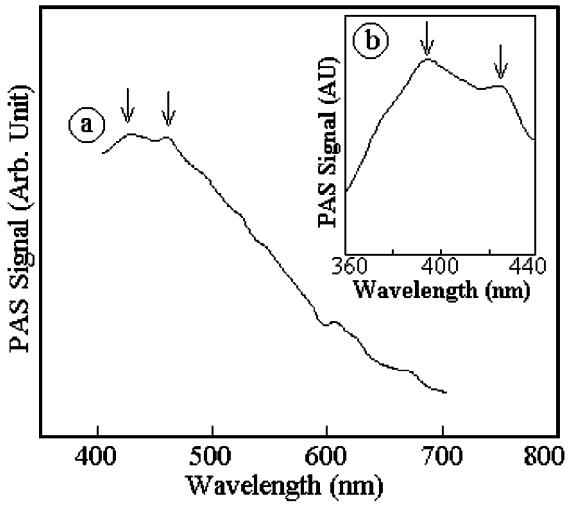

Figure 7. Photoacoustic spectra of (a) crystalline silver nanoparticles deposited on silica submicrospheres, sample 2h, and (b) sample 1h (spectrum magnified 5 times).

Again two peaks are observed, but their intensity decreased, and the peaks are blue shifted to 394 and 424 nm, relative to sample 2h. This blue shift was attributed by Weiping et al.[30] to the oxidation of silver to silver oxide. This hypothesis is consistent with our results, which showed that sample 1h is a Ag/Ag_2O mixture (see Figure 1b). Furthermore, the oxidation reduces the quantity of Ag, thus reducing the intensity. Here also, two types of particles were detected.

On the basis of these results, we conclude that the PAS technique can be used for SPR measurements, and it is much more sensitive than classical absorption spectroscopy (no peaks were detected at all with sample 1h using the UV−vis absorption method).

7. Fourier Transform Infrared (FT-IR) Studies. FT-IR absorption of the various reactive species on the surface of silica may be used in order to assess the extent of interaction between the metal and the surface. This interaction may drastically change the nature of the precipitate. For example, Fe coated on silica surfaces immediately oxidizes.[14] In other cases, for example, Ni, the oxidation does not occur.[15] The FT-IR spectra of the bare SiO_2 spheres as well as amorphous Ag/SiO_2 and Ag/SiO_2 particles (samples 2 and 2h, respectively) are shown in Figure 8a−c. One of the main changes between these spectra is a decrease in the intensity of the peaks in the broad 900−1300 cm^{-1} range for the surface-deposited samples. This range corresponds to the asymmetric stretching (AS) vibration mode of the Si−O−Si bridge of the siloxane link.[31] Also, a relatively strong peak at 805−810 cm^{-1}, which is observed in Figure 8a and corresponds to the symmetric stretching of the Si−O−Si group, completely disappears from the spectra of both coated samples. This result might be explained as follows. During a sonochemical reaction, the energy produced during bubble collapse is sufficient to rupture the strained surface Si−O−Si bonds. This activates the surface of the silica spheres, producing better adhesion of the formed silver nanoparticles. A similar kind of surface modification of the silica core was also observed in other systems.[32] We suggest that as in our previous studies[12−15] a Ag−O−Si bond is created; this bond would appear below 400 cm^{-1}.

(31) Kirk, C. T. *Phys. Rev. B* **1988**, *38*, 1255−1273.
(32) Patra, A.; Sominska, E.; Ramesh, S.; Koltypin, Y.; Zhong, Z.; Minti, H.; Reisfeld, R.; Gedanken, A. *J. Phys. Chem. B* **1999**, *103*, 3361−3365.

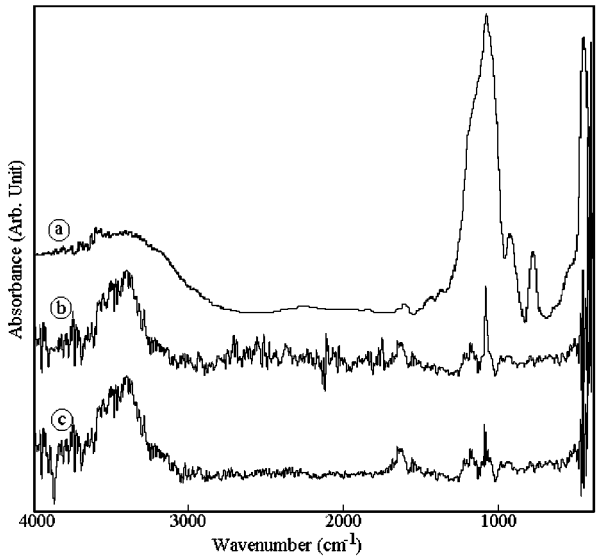

Figure 8. FT-IR spectra of (a) the bare substrate silica spheres, (b) sample 2, and (c) sample 2h.

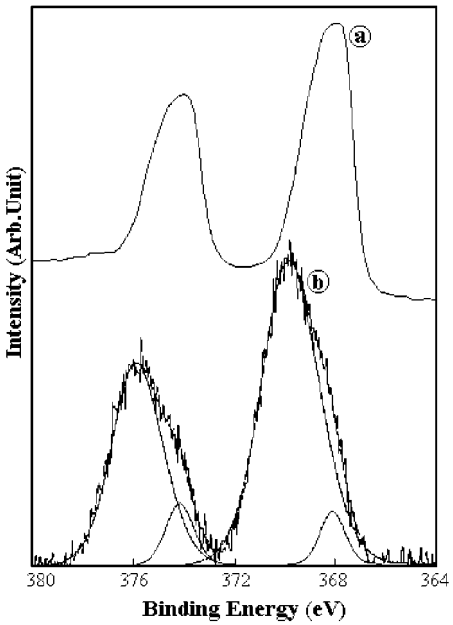

Figure 9. X-ray photoelectron spectra of the Ag 3d transition: (a) crystalline silver nanoparticles deposited on silica submicrospheres with bubbling argon gas prior to sonication (sample 2h) and (b) silver nanoparticles deposited on silica submicrospheres without bubbling argon gas prior to sonication (sample 1h).

8. X-ray Photoelectron Spectroscopy (XPS). XPS spectra of the crystalline silver-coated silica submicrospheres, recorded in the energy region of the Ag 3d transition, are presented in Figure 9a,b (samples 2h and 1h, respectively). For sample 1h, the observed peaks were asymmetric in shape, and a deconvolution procedure for this spectrum was used in order to determine the exact position of the peaks. In Figure 9a, the metallic Ag 3d peaks are centered at 367.9 and 373.9 eV, while Figure 9b shows Ag_2O peaks at 369.6 and 375.8 eV. The positions of these peaks are in agreement with published data.[30] The ratio of the areas of both doublets in Figure 9b indicates that much more silver oxide than silver is present on the surface of the sample. This result appears to contradict the XRD results (see Figure 1b) which show that more silver than silver oxide is present in the sample. This result might be explained by the fact that in composite

Ag/Ag_2O nanoparticles, silver oxide mainly occurs on the surface of the particles, while the core is mainly silver. Since XPS is a surface analytical method (penetration depth is approximately 1−2 nm),[33] it detects the Ag_2O more readily than the Ag. Even in the case of small nanoparticles (1−5 nm), XPS primarily probes the surface of these nanoparticles. On the other hand, XRD is a method of bulk analysis with much higher penetration depth, which therefore probes both Ag_2O and Ag equally.

For sample 2h (see Figure 9a), only one species was observed (metallic silver), in agreement with the XRD data.

Sonochemical Reaction/Mechanism for the Deposition of Silver Nanoparticles on Silica Submicrospheres

The chemical reactions can be driven by intense ultrasonic waves, which are strong enough to produce oxidation, reduction, dissolution, and decomposition.[34−36] Three different regions are formed[37] during an aqueous sonochemical process: (a) the inner environment (gas phase) of the collapsing bubbles, where elevated temperatures (several thousands of degrees) and pressures (hundreds of atmospheres) are produced, causing water to pyrolyze into H and OH radicals; (b) the interfacial region where the temperature is lower than in the gas-phase region but still high enough to induce a sonochemical reaction (a few hundred degrees Celsius); and (c) the bulk solution, which is at ambient temperature. Sonochemical reactions appear to occur within the interfacial region. To test this hypothesis, a number of control experiments were conducted. In a control reaction, silica, $AgNO_3$, NH_3, and Ar/H_2 in the same ratio were vigorously stirred in an aqueous solution, without sonication, and no silver nanoparticles were obtained. A second control experiment was carried out with the same reagents, without sonication but with regular heating (refluxing for a few hours). In this case, a few silver particles were observed, but the silica spheres remained uncoated, thus showing that temperatures higher than 100 °C are required for this reaction. The temperatures, which are attributed to the inner environment of the bubble or interfacial region, are in fact much higher than 100 °C. Because no Ag^+ ions could be inside the collapsing bubble (in the gas phase), we conclude that the formation of the silver nanoparticles occurs in the interfacial region. The low abundance of silver ions in the ∼200 nm bubble ring is the reason for the formation of nanoparticles.

This mechanism of the formation of silver nanoparticles takes into consideration that free radical species are generated from water molecules by the absorption of ultrasound (eq 1). This would be the initiation reaction.

$$H_2O \text{))))))) } H^\bullet + {}^\bullet OH \quad (1)$$

The H radical formed in eq 1 can act as a reducing species and trigger the reduction (eq 2):

$$Ag^+ + H^\bullet = Ag^0 + H^+ \quad (2)$$

The sonochemical reduction process generates high temperatures and pressures for the reduction of $AgNO_3$ to amorphous silver.[16] An argon/hydrogen mixture produces even more H radicals, thus enhancing the reduction of Ag^+ under the sonochemical conditions (propagation of the reaction; in reactions without H_2, with only Ar, almost no silver was formed). In the presence of ammonia, the reaction may be modified to

$$Ag^+ + 2NH_3 \rightarrow Ag(NH_3)_2^+ \quad (3)$$

$$2Ag(NH_3)_2^+ + H^\bullet \rightarrow 2Ag_{(S)} + (NH_4)^+ + NH_3 \quad (4)$$

Ammonia can activate the SiO_2 surface to produce reactive silanol groups. It is possible that a moderately strong chemical bond between the siloxane oxygen and elemental Ag ($Si-O-Ag^{\delta+}$) is formed. A theoretical investigation by Johnson and Pepper[38] showed that the formation of a direct and primarily covalent chemical bond between an elemental metal such as Fe, Ni, Cu, or Ag and oxygen anions on the surface of clean sapphire is favored. Alternatively, NH_3 might form a stable $(Ag(NH_3)_2)^+$ complex, which can be attracted to the partially negatively charged SiO_2 spheres, which after sonication produce bonded Ag on SiO_2. This is supported by a reaction in which silica, $AgNO_3$, and Ar/H_2 in the same ratio were sonicated in the absence of ammonia in an aqueous solution. Only a few of the resulting silver particles coat the silica surface, while the major part of the silver particles are separated from that surface. The silica spheres were not fully coated, as in the sonication process in the presence of ammonia. The mechanism by which the silver nanoparticles are bonded to the silica surface is related to the microjets and shock waves created after the collapse of the bubble.[39] These jets, which cause, for example, the sintering of micron-sized metallic particles, push the nanoparticles toward the silica surface at very high speeds. When they hit the silica surface, they can react with free silanols, or even Si−O−Si bonds. This may result in adhesion of the nanoparticles to the silica even when they were not formed on the SiO_2 surface.

Conclusions

Nanoparticles of silver, ∼5 nm in size, were deposited by ultrasound on the surface of submicrospheres of silica from a basic aqueous solution containing Ag^+ ions. The advantages of the process described in this report are that it is simple and efficient and produces a uniform coating of silver nanoparticles on the silica submicrospheres. The period of sonication is only 90 min as compared with other methods which take a minimum of 140,[6] 15,[7] or 24 h.[8] The importance of bubbling argon gas for 4 h prior to sonication is emphasized. If the oxygen is not removed, a silver oxide/silver mixture is obtained. As far as we know, this is first complete study of the silica surface coated with silver nanoparticles. In the few earlier studies, only a limited number of the characterization techniques were used.[6−8]

Acknowledgment. V. G. Pol is thankful to the President's Fund of Bar-Ilan University, Israel, for financial assistance. The authors thank Y. Gofer and G. Salitra for XPS measurements.

LA0155552

(33) *Surface analysis*: *The principal techniques*; Vickerman, J. C., Ed.; Wiley: Chichester, 1997.

(34) Suslick, K. S.; Choe, S. B.; Cichowlas, A. A.; Grinstaff, M. W. *Nature* **1991**, *353*, 414−416.

(35) Gutierrez, M.; Henglein, A.; Dohrmann, J. *J. Phys. Chem.* **1987**, *91*, 6687−6690.

(36) Alegria, A. E.; Lion, Y.; Kondo, T.; Riesz, P. *J. Phys. Chem.* **1989**, *93*, 4908−4913.

(37) Suslick, K. S.; Hammerton, D. A. *IEEE Trans. Sonics Ultrason.* **1986**, *SU-33*, 143−147.

(38) Johnson, K. H.; Pepper, S. V. *J. Appl. Phys.* **1982**, *53*, 6634−6638.

(39) Suslick, K. S.; Price, G. J. *Annu. Rev. Mater. Sci.* **1999**, *29*, 295−326.